集された、若年者ヒトDPSC は、ヒトHDFと比較して、少ない因子の導入によって、高い効率でiPS 細胞に誘導できた。今回は、遺伝子挿入のあるレトロウイルスベクターを用いたが、近年報告が相次いでいる遺伝子改変を伴わない誘導法によってiPS 細胞バンクの構築をおこなう際にも、有用なリソースとなるだろう。また、今回DPSC コレクション内に見つかった２例のHLA-A, B, DR ローカスホモのラインについては、優先的にiPS 細胞誘導を行い，現在その性状を確認している。今回取り出されたDPSC から、高い効率と少ない因子導入でiPS 細胞が誘導できた事から、われわれの細胞コレクションはがん幹細胞を標的とした遺伝子治療のモデルとして多数の日本人のiPS細胞を供給可能である。さらに、iPS 細胞細胞から各種がん幹細胞を誘導する試みがなされており、このような技術の進展に伴って我々の作成したiPS細胞の利用価値が高まると予想される。

E.結論

1） 岐阜大学医学部で収集した歯髄幹細胞(DPSC)約１８０人分の細胞を培養し、保存した。

2） これらの歯髄細胞に山中因子をレトロウイルスおよびセンダイウイルスベクターを用いて導入し，iPS細胞を誘導した。

F．健康危険情報

特になし

G．研究発表

1. 論文発表

1) Hara, A, Taguchi A, Aoki H, Hatano Y, Niwa M, Yamada Y, Kunisada T. Folate antagonist, methotrexate induces neuronal differentiation of human embryonic stem cells transplanted into nude mouse retina. Neurosci Lett. 477, 138-143, 2010.

2) Iida K, Takeda-Kawaguchi T, Tezuka Y, Kunisada T, Shibata T, Tezuka K. Hypoxia enhances colony formation and proliferation but inhibits differentiation of human dental pulp cells. Arch Oral Biol. 55, 648-654. 2010.

3) Tamaoki N, Takahashi K, Tanaka T, Ichisaka T, Aoki H, Takeda-Kawaguchi T, Iida K, Kunisada T, Shibata T, Yamanaka S, Tezuka K. Dental pulp cells for induced pluripotent stem cell banking. J Dent Res. 89, 773-778, 2010.

4) Aoki H, Hara A, Motohashi T, Osawa M, Kunisada T. Functionally distinct melanocyte populations revealed by reconstitution of hair follicles in mice. Pigment Cell Melanoma Res. 24, 125-135, 2011.

5) Walker GJ, Soyer HP, Handoko HY, Ferguson B, Kunisada T, Khosrotehrani K, Box NF, Muller HK. Superficial Spreading-Like Melanoma in Arf(-/-)::Tyr-Nras(Q61K)::K14-Kitl Mice: Keratinocyte Kit Ligand Expression Sufficient to "Translocate" Melanomas from Dermis to Epidermis. J Invest Dermatol. in press.

2. 学会発表

1) 青木仁美、國貞隆弘、色素細胞幹細胞への遺伝毒性ストレスに対する色素細胞分化増殖因子の影響、第 23 回日本色素細胞学会学術大会 慈恵医科大学(東京),2010年11月27日

2) 手塚 建一, 玉置 也剛、高橋 和利、柴田 敏之、國貞 隆弘、山中 伸弥、HLA ハプロタイプホモ iPS 細胞バンクのための歯髄細胞バンク利用 2（1岐阜大・組織・器官形成、第33回日本分子生物学会年会第83回日本生化学会大会合同大会、2010年12月10日

3) 玉置 也剛 高橋和利 柴田敏之 國貞隆弘 山中伸弥 手塚建一、iPS細胞バンクのリソースとしてのヒト歯髄細胞の有用性、第10回日本再生医療学会、東京、2011年3月２日

4）本橋 力 若岡敬紀 北川大輔 國貞隆弘、マウス内耳由来神経堤細胞の多分化能の解析、第10回日本再生医療学会、東京、2011年3月1日

H.知的財産権の出願・登録状況（予定を含む。）

1. 特許取得

なし

2. 実用新案登録
なし

3. その他
なし

厚生労働科学研究費補助金（第３次対がん総合戦略研究事業）
分担研究報告書

人工グリオーマ幹細胞を用いた癌幹細胞制御機構の解明

研究分担者　　近藤　亨　愛媛大学プロテオ医学研究センター（幹細胞部門）・教授

研究要旨
私たちは、癌幹細胞の性状を明らかにするために試験管内で癌幹細胞を作製する方法を樹立した。神経幹細胞とオリゴデンドロサイト前駆細胞から誘導した人工グリオーマ幹細胞は、免疫不全マウス脳内に移植することにより、ヒトグリオブラストーマ(GBM、膠芽腫)と同じ病理所見を示す悪性脳腫瘍を形成する。この人工グリオーマ幹細胞、ヒト GBM と退形成性乏突起膠腫(AO)から樹立したグリオーマ幹細胞株、ヒトグリオーマ組織サンプルを用いて、新規グリオーマ治療標的因子を探索した。その結果、Cox2 と EGF 受容体リガンドの発現がグリオーマ幹細胞で増加し、両因子に対する阻害剤の組合せがオリゴデンドロサイト系譜細胞から由来するグリオーマの腫瘍形成能を抑制することを見いだした。

A.研究目的

腫瘍に存在する癌幹細胞は、幹細胞能力・腫瘍形成能・治療抵抗性を有する。このため癌幹細胞を正しく性状解析し治療標的を同定することが、癌根治療法の創出に繋がる。私たちは試験官内で癌幹細胞の作製を試み、神経幹細胞とオリゴデンドロサイト前駆細胞を起源とするグリオーマ幹細胞の作製に成功した。この人工グリオーマ幹細胞は、１０個をヌードマウス脳内に移植することによりヒト GBM と同じ病理所見を示す悪性脳腫瘍を形成する。(Hide et al, Cancer Res. 2009; Nishide et al, PLoS One 2009; Hide et al, Stem Cells 2011)。本研究では、この人工グリオーマ幹細胞を用いて、新規グリオーマ治療標的および治療方法を検討した。

B.研究方法

現在までに人工グリオーマ幹細胞とその親株間での遺伝子発現プロファイルから人工グリオーマ幹細胞に優位に発現している遺伝子群を同定し、ヒトグリオーマ幹細胞株とヒトグリオーマ組織サンプルを用いて候補遺伝子の発現を検証し、複数の治療標的因子群を同定していた。その中で既に治療薬として認可のおりている薬剤の標的となっている因子群に研究標的を絞り、それら薬剤の組合せがグリオーマ治療に有効であるかどうかについて、試験管内実験、移植実験により検討した。

C.研究結果

本研究により、グリオーマ幹細胞が Cox2 と各種 EGF 受容体リガンドを高発現していることを見いだした。更にオリゴデンドロサイト系譜から由来するグリオーマ幹細胞は、両シグナルに依存性が高く、これらシグナル伝達を阻害する経口薬 Celecoxib と Gefitinib の併用によりその腫瘍形成能を阻害できることが明らかとなった。一方、神経幹細胞由来グリオーマ幹細胞は、これら阻害剤に明らかな感受性を示さなかった。

D.考察

グリオーマは、その形状と特異的な免疫染色性により病理分類されているが、最も悪性度の高い GBM では、多種多様な細胞が混在していること、その判断基準（ネクローシス、血管新生、多核細胞の存在等）からその起源細胞を特定することは難しい。今回の研究成果は同じ病理所見を有する GBM において、その起源細胞の違いにより治療標的が異なる事を明らかにした。今後様々な腫瘍において、その癌幹細胞の起源候補細胞に癌遺伝子／癌抑制遺伝子変異を導入し、人工癌幹細胞を作製し、それぞれの癌幹細胞のマーカーの同定や既存／新規薬剤の効果を検討する必要がある。

F．健康危険情報　　なし

G．研究発表

1．論文発表

1) Inoda, S., Hirohashi, Y., Torigoe, T., Morita, R., Takahashi, A., Asanuma, H., Nakatsugawa, M., Nishizawa, S., Tamura, Y., Tsuruma, T., Terui, T., Kondo, T., Ishitani, K., Hasegawa, T., Hirata, K., & Sato, N. (2011). Cytotoxic T lymphocytes efficiently recognize human colon cancer stem-like cells. **Am. J. Pathol.** 178, 1805-1813.

2) Hide, T., Takezaki, T., Nakatani, Y., Nakamura, H., Kuratsu, J., & Kondo, T. (2011). Combination of a Ptgs2 inhibitor and an EGFR signaling inhibitor prevents tumorigenesis of oligodendrocyte-lineage derived glioma-initiating cells. **Stem Cells** 29, 590-599.

3) 近藤　亨（2010）. カラー図説:癌幹細胞と分子標的薬。固形癌の最新治療- 癌治療への新たな取り組み- 日本臨床社 68, 986-990.

4) 近藤　亨（2010）. 人工グリオーマからの考察。再生医療、メディカルレビュー社 9, 42-46.

5) 近藤　亨（2010）. 幹細胞生物学からみた脳腫瘍の発生機序。新時代の脳腫瘍学- 診断・治療の最前線- 日本臨床社 増刊号 68, 24-28.

6) Kondo T. (2010). Mouse induced glioma-initiating cell models and therapeutic targets. Anticancer agents Med. Chem. 10, 471-480.

7) 近藤　亨 (2010). 膠芽腫。Clinical Neuroscience 28, 1419-1421.

2. 学会発表

1) 近藤　亨（2010）　グリオーマ幹細胞の性状解析。第５１回日本臨床細胞学会　シンポジウム　横浜

2) 近藤　亨 (2010) Cancer stem cell と標的分子。第１４回日本がん分子標的治療学会　Year in Review　東京

3) Toru Kondo. (2010) Induced glioma-initiating cell models reveal novel therapeutic targets. 15th World Congress on Advances in Oncology&13th International Symposium on Molecular Medicine. Invited speaker. Greece.

4) Toru Kondo. (2011) Making of glioma-initiating cell models and searching for their novel therapeutic targets. 高度医療都市を創出する未来技術国際シンポジウム　岡山

H. 知的財産権の出願・登録状況

1. 特許取得予定

なし

2. 実用新案登録

なし

別紙４

研究成果の刊行に関する一覧表

書籍

著者氏名	論文タイトル名	書籍全体の編集者名	書　籍　名	出版社名	出版地	出版年	ページ

雑誌

発表者氏名	論文タイトル名	発表誌名	巻号	ページ	出版年
Khai NC, Sakamoto K, Takamatsu H, Matsuura H, Kosai K.	Recombinant soluble form of HB-EGF protein therapy drastically inhibits Fas-mediated fulminant hepatic failure: Implications in clinical application.	Hepatol Res	*in press*		2011
Okabe Y, Kusanaga A, Takahashi T, Mitsumasu C, Murai Y, Tanaka E, Higashi H, Matsuishi T, Kosai K.	Neural Development of Methyl-CpG-Binding Protein 2 Null Embryonic Stem Cells: A System for Studying Rett Syndrome.	Brain Res	1360	17-27	2010
Miyata S, Takemura G, Kosai K, Takahashi T, Esaki M, Li L, Kanamori H, Maruyama R, Goto K, Tsujimoto A, Takeyama T, Kawaguchi T, Ohno T, Nishigaki K, Fujiwara T, Fujiwara H, Minatoguchi S	Anti-Fas Gene Therapy Prevents Doxorubicin-induced Acute Cardiotoxicity through Mechanisms Independent of Apoptosis.	Am J Pathol	176(2)	687-698	2010
Wang Y, Asakawa A, Inui A, Kosai K.	Leptin gene therapy in the fight against diabetes.	Expert.Opin.Biol.Ther	10(10)	1405-1414	2010
Matsunoshita Y, Ijiri K, Ishidou Y, Nagano S, Yamamoto T, Nagao H, Komiya S, Setoguchi T.	Suppression of Osteosarcoma Cell Invasion by Chemotherapy Is Mediated by Urokinase Plasminogen Activator Activity via Up-Regulation of EGR1.	PLoS ONE.	6(1)		2011
Nagao H., Ijiri K., Hirotsu M., Ishidou Y., Yamamoto T., Nagano S., Takizawa T., Nakashima K., Komiya S., and Setoguchi T.	Role of GLI2 in the growth of human osteosarcoma.	The Journal of Pathology	224	1-11	2011

Otsuka H, Arimura N, Sonoda S, Nakamura M, Hashiguchi T, Maruyama I, Nakao S, Hafezi-Moghadam A, Sakamoto T.	Stromal cell-derived factor-1 is essential for photoreceptor cell protection in retinal detachment.	Am J Pathol.	177(5)	2268-2277	2010
Shrestha B, Hashiguchi T, Ito T, Miura N, Takenouchi K, Oyama Y, Kawahara K, Tancharoen S, Ki-I Y, Arimura N, Yoshinaga N, Noma S, Shrestha C, Nitanda T, Kitajima S, Arimura K, Sato M, Sakamoto T, Maruyama I.	B cell-derived vascular endothelial growth factor A promotes lymphangiogenesis and high endothelial venule expansion in lymph nodes.	J Immunol.	184(9)	4819-4826	2010
Kase S, He S, Sonoda S, Kitamura M, Spee C, Wawrousek E, Ryan SJ, Kannan R, Hinton DR	alphaB-crystallin regulation of angiogenesis by modulation of VEGF.	Blood.	115(16)	3398-3406	2010
JP Yang, R. Yoshida, Y. Kariya, X. Zhang, S. Hashiguchi, T. Nakashima, Y. Suda, A. Takada, Y. Ito and K. Sugimura	Characterization of human single-chain antibodies against highly pathogenic avian influenza H5N1 viruses: mimotope and neutralizing activity	The Journal of Biochemistry	148(4)	507-515	2010
E. Wijelath, M. Namekata, J. Murray, M. Furuyashiki, S. Zhang, D. Coan, M. Wakao, R. B. Harris, Y. Suda, L. Wang, M. Sobel.	Multiple mechanisms for exogenous heparin modulation of vascular endothelial growth factor activity	Journal of Cellular Biochemistry	111(2)	461-468	2010
H. Kariya, Y. Yoshihara, Y. Nakao, N. Sakurai, M. Ueno, M. Hashimoto, Y. Suda	Carboxymethyl-chitin promotes chondrogenesis by inducing the production of growth factors from immune cells.	Journal of Biomedical Materials Research Part A	94A(4)	1034-1041	2010
Tamaoki N, Takahashi K, Tanaka T, Ichisaka T, Aoki H, Takeda-Kawaguchi T, Iida K, Kunisada T, Shibata T, Yamanaka S, Tezuka K.	Dental pulp cells for induced pluripotent stem cell banking.	J Dent Res	89	773-778	2010
Aoki H, Hara A, Motohashi T, Osawa M, Kunisada T.	Functionally distinct melanocyte populations revealed by reconstitution of hair follicles in mice.	Pigment Cell Melanoma Res.	24	125-135	2011

Inoda, S., Hirohashi, Y., Torigoe, T., Morita, R., Takahashi, A., Asanuma, H., Nakatsugawa, M., Nishizawa, S., Tamura, Y., Tsuruma, T., Terui, T., Kondo, T., Ishitani, K., Hasegawa, T., Hirata, K., & Sato, N.	Cytotoxic T lymphocytes efficiently recognize human colon cancer stem-like cells.	Am. J. Pathol.	178	1805-1813	2011
Hide, T., Takezaki, T., Nakatani, Y., Nakamura, H., Kuratsu, J., & Kondo, T.	Combination of a Ptgs2 inhibitor and an EGFR signaling inhibitor prevents tumorigenesis of oligodendrocyte-lineage derived glioma-initiating cells.	StemCells	29	590-599	2011

Hepatology Research

Hepatology Research 2011; **41**: 594–596 doi: 10.1111/j.1872-034X.2011.00805.x

Letter to the Editor

Recombinant soluble form of heparin-binding epidermal growth factor-like growth factor protein therapy drastically inhibits Fas-mediated fulminant hepatic failure: Implications in clinical application

The mRNA levels of heparin-binding epidermal growth factor-like growth factor (HB-EGF) increased more rapidly than those of hepatocyte growth factor (HGF), the well-studied hepatotropic factor, in regenerating livers after a partial hepatectomy and liver injury.[1–6] The membrane-anchored precursor form (proHB-EGF) is initially synthesized in non-parenchymal cells, and the extracellular domain is cleaved by a specific metalloproteinase.[7,8] The resulting soluble form of HB-EGF (sHB-EGF) acts on neighboring hepatocytes.[1,9] Our previous study demonstrated the therapeutic effects of proHB-EGF gene (pHB-EGFg) therapy in liver disease.[9] The recombinant human sHB-EGF protein (rsHB-EGFp) therapy remains to be studied because it is potentially more clinically suited to inhibit fulminant hepatic failure than pHB-EGFg therapy due to its instant action (i.e. no time lag as in pHB-EGFg therapy, such as proHB-EGF transcription and translation and the subsequent shedding of sHB-EGF in hepatocytes) and the feasibility to terminate treatment, and because the modes of actions may differ between pHB-EGFg and rsHB-EGFp therapies. The present study examines the ability of the rsHB-EGFp therapy to inhibit fulminant hepatic failure in mice.

The initial and essential event in many liver diseases, particularly acute viral hepatitis and the subsequent fulminant hepatic failure, is excessive activation of the Fas system.[4,9,10] Five- to six-week-old male C57BL/6J mice ($n = 8$ per group) were administrated three i.p. injections of 100 μg/mouse rsHB-EGFp at 6 and 0.5 h before and 3 h after the mice were i.p. injected with 4 μg/mouse of an agonistic anti-Fas antibody (4Fas-ip) as previously described.[4,9] Twenty-four hours after administrating 4Fas-ip, the serum alanine aminotransferase (ALT), aspartate aminotransferase (AST) and lactate dehydrogenase (LDH) levels were remarkably increased in the control saline-treated mice (2853 ± 814, 1817 ± 469 and 3782 ± 1222 IU/L, respectively) (Fig. 1a), but were drastically attenuated to normal levels in the rsHB-EGFp-treated mice (ALT, 21 ± 5; AST, 28 ± 4; LDH, 119 ± 16 IU/L). Accordingly, all of the control mice had histopathological liver injury, including apoptosis, while none of the rsHB-EGFp-treated mice had histopathological findings of liver injury 24 h after 4Fas-ip was administrated (Fig. 1b,c). rsHB-EGFp treatment significantly reduced Bax expression, whereas Bcl-2 or Bcl-xl expression was unaffected (Fig. 1d). Because Bax and Bcl-2/Bcl-xl positively and negatively regulate apoptosis, respectively, this result further suggests that rsHB-EGFp therapy ameliorated apoptotic properties.

In survival analyses, four of six (67%) control mice died within 17 h, and only two of six (33%) mice survived up to 48 h after they had received 8 μg/mouse of Fas-ip (8Fas-ip) (Fig. 1e). In contrast, all rsHB-EGFp-treated mice survived up to 48 h after receiving 8Fas-ip.

Our findings and the previous studies revealed that rsHB-EGFp pharmacotherapy elicited greater protective effects than hepatic pHB-EGFg therapy in inhibiting fulminant hepatic failure, because the latter greatly but not completely attenuated liver injury.[9] This difference may be due to the lack of vector-related hepatotoxicity and to direct actions in rsHB-EGFp therapy. Although additional studies should be performed, these promising results and the lack of effective medicines that radically inhibit fulminant hepatic failure indicate that

Correspondence: Dr Ken-ichiro Kosai, Department of Gene Therapy and Regenerative Medicine, Kagoshima University Graduate School of Medical and Dental Sciences, 8-35-1 Sakuragaoka, Kagoshima, 890-8544, Japan. Email: kosai@m2.kufm.kagoshima-u.ac.jp

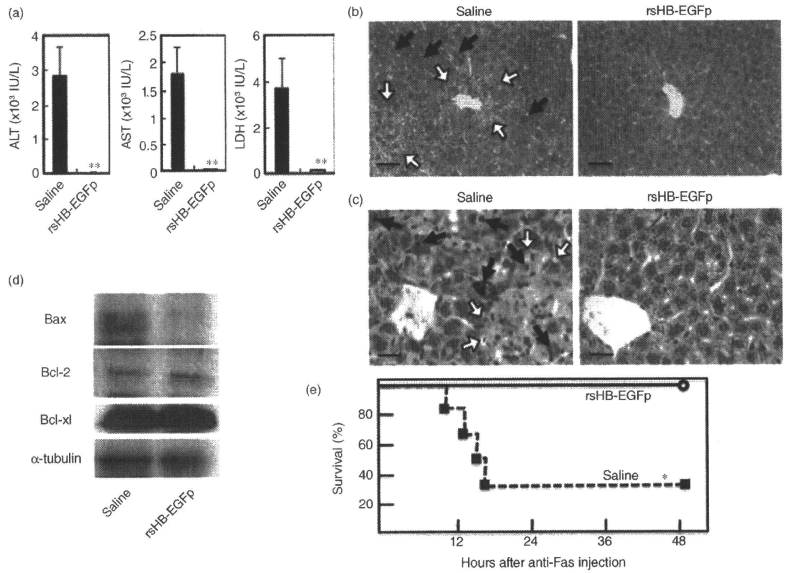

Figure 1 Therapeutic effects of recombinant human soluble form of heparin-binding epidermal growth factor-like growth factor protein (rsHB-EGFp) pharmacotherapy in inhibiting Fas-mediated fulminant hepatic failure in mice. Mice were administrated 4 μg/mouse of an agonistic anti-Fas antibody i.p. (4Fas-ip) (a–d) or 8 μg/mouse of an agonistic anti-Fas antibody i.p. (8Fas-ip) (e) at 0 h and i.p. injections of rsHB-EGFp or saline at −6, −0.5 and 3 h. (a) The serum alanine aminotransferase (ALT), aspartate aminotransferase (AST) and lactate dehydrogenase (LDH) levels at 24 h after 4Fas-ip were drastically increased in the saline-treated control mice, but were virtually normal in the rsHB-EGFp-treated mice. All data are expressed as the mean ± standard error (**$P < 0.01$). (b) Hematoxylin–eosin-stained liver histology sections of the rsHB-EGFp-treated or saline-treated mice 24 h after was administrated 4Fas-ip (scale bar, 100 μm). Histopathological findings of liver injury (e.g. apoptosis [black arrows] and swollen hepatocytes [white arrows]) were observed in the saline-treated mice but not in the rsHB-EGFp-treated mice. (c) Terminal deoxynucleotidyl transferase-mediated deoxyuridine triphosphate nick end labeling (TUNEL)-positive apoptotic cells (black arrows) and clusters of dead hepatocytes (white arrows) were conspicuously found only in the saline-treated mice (scale bar, 50 μm). (d) Western blot analysis of Bax, Bcl-2, Bcl-xl and α-tubulin (internal control) in liver tissues from saline-treated or rsHB-EGFp-treated mice 24 h after 4Fas-ip was administrated. (e) A Kaplan–Meier analysis showed survival differences between the two groups ($n = 6$ per group) (*$P < 0.05$), and all of the rsHB-EGFp-treated mice survived up to 48 h after receiving 8Fas-ip.

rsHB-EGFp pharmacotherapy should be rapidly developed as a clinical therapy.

Ngin Cin Khai,[1] Kouichi Sakamoto,[1,2] Hideo Takamatsu,[3] Hiroshi Matsufuji[2] and Ken-ichiro Kosai[1]

Departments of [1]Gene Therapy and Regenerative Medicine and [2]Pediatric Surgery, Kagoshima University Graduate School of Medical and Dental Science, and [3]Kagoshima University Medical and Dental Hospital, Kagoshima, Japan

REFERENCES

1 Kiso S, Kawata S, Tamura S *et al.* Expression of heparin-binding EGF-like growth factor in rat liver injured by carbon tetrachloride or d-galactosamine. *Biochem Biophys Res Commun* 1996; **220**: 285–8.

2 Kiso S, Kawata S, Tamura S *et al.* Role of heparin-binding epidermal growth factor-like growth factor as a hepatotrophic factor in rat liver regeneration after partial hepatectomy. *Hepatology* 1995; **22**: 1584–90.

3 Kosai K, Matsumoto K, Funakoshi H, Nakamura T. Hepatocyte growth factor prevents endotoxin-induced lethal hepatic failure in mice. *Hepatology* 1999; **30**: 151–9.

4 Kosai K, Matsumoto K, Nagata S, Tsujimoto Y, Nakamura T. Abrogation of Fas-induced fulminant hepatic failure in mice by hepatocyte growth factor. *Biochem Biophys Res Commun* 1998; **244**: 683–90.

5 Kosai KI, Finegold MJ, Thi-Huynh BT *et al.* Retrovirus-mediated in vivo gene transfer in the replicating liver using recombinant hepatocyte growth factor without liver injury or partial hepatectomy. *Hum Gene Ther* 1998; **9**: 1293–301.

6 Ido A, Moriuchi A, Marusawa H *et al.* Translational research on HGF: a phase I/II study of recombinant human HGF for the treatment of fulminant hepatic failure. *Hepatol Res* 2008; **38**: S88–S92.

7 Kimura R, Iwamoto R, Mekada E. Soluble form of heparin-binding EGF-like growth factor contributes to retinoic acid-induced epidermal hyperplasia. *Cell Struct Funct* 2005; **30**: 35–42.

8 Higashiyama S. Metalloproteinase-mediated shedding of heparin-binding EGF-like growth factor and its pathophysiological roles. *Protein Pept Lett* 2004; **11**: 443–50.

9 Khai NC, Takahashi T, Ushikoshi H *et al.* In vivo hepatic HB-EGF gene transduction inhibits Fas-induced liver injury and induces liver regeneration in mice: a comparative study to HGF. *J Hepatol* 2006; **44**: 1046–54.

10 Oksuz M, Akkiz H, Isiksal YF *et al.* Expression of Fas antigen in liver tissue of patients with chronic hepatitis B and C. *Eur J Gastroenterol Hepatol* 2004; **16**: 341–5.

BRAIN RESEARCH 1360 (2010) 17–27

available at www.sciencedirect.com

ScienceDirect

www.elsevier.com/locate/brainres

BRAIN RESEARCH

Research Report

Neural development of methyl-CpG-binding protein 2 null embryonic stem cells: A system for studying Rett syndrome

Yasunori Okabe[a,b,1], Akira Kusaga[a,c,1], Tomoyuki Takahashi[a,d,1], Chiaki Mitsumasu[a,c], Yoshinaka Murai[b], Eiichiro Tanaka[a,b], Hideho Higashi[b], Toyojiro Matsuishi[a,c], Ken-ichiro Kosai[a,c,e,*]

[a]Division of Gene Therapy and Regenerative Medicine, Cognitive and Molecular Research Institute of Brain Diseases, Kurume University, Kurume, Japan
[b]Department of Physiology, Kurume University of Medicine, Kurume, Japan
[c]Department of Pediatrics, Kurume University of Medicine, Kurume, Japan
[d]Department of Advanced Therapeutics and Regenerative Medicine, Kurume University of Medicine, Kurume, Japan
[e]Department of Gene Therapy and Regenerative Medicine, Advanced Therapeutics Course, Kagoshima University Graduate School of Medical and Dental Sciences, Kagoshima, Japan

ARTICLE INFO

Article history:
Accepted 27 August 2010
Available online 25 September 2010

Keywords:
MeCP2
Rett syndrome
Embryonic stem cell
Adenoviral vector

ABSTRACT

Mutations in methyl-CpG-binding protein 2 (MeCP2) gene cause the neurodevelopmental disorder Rett syndrome (RTT). Here, we describe a new experimental system that efficiently elucidates the role of MeCP2 in neural development. MeCP2-null and control ES cells were generated by adenoviral conditional targeting and examined for maintenance of the undifferentiated ES cell state, neurogenesis, and gliogenesis during *in vitro* differentiation. In addition, dopamine release and electrophysiological features of neurons differentiated from these ES cells were examined. Loss of MeCP2 did not affect undifferentiated ES cell colony morphology and growth, or the timing or efficiency of neural stem cell differentiation into Nestin-, TuJ- or TH-positive neurons. In contrast, gliogenesis was drastically accelerated by MeCP2 deficiency. Dopamine production and release in response to a depolarizing stimulus in MeCP2-null ES-derived dopaminergic neurons was intact. However, MeCP2-null differentiated neurons showed significantly smaller voltage-dependent Na^+ currents and A-type K^+ currents, suggesting incomplete maturation. Thus, MeCP2 is not essential for maintenance of the undifferentiated ES cell state, neurogenesis, or dopaminergic function; rather, it is principally involved in inhibiting gliogenesis. Altered neuronal maturity may indirectly result from abnormal glial development and may underlie the pathogenesis of RTT. These data contribute to a better understanding of the developmental roles of MeCP2 and the pathogenesis of RTT.

* *Corresponding author.* Department of Gene Therapy and Regenerative Medicine, Advanced Therapeutics Course, Kagoshima University Graduate School of Medical and Dental Sciences, 8-35-1 Sakuragaoka, Kagoshima 890-8544, Japan. Fax: +81 9 265 9721.
E-mail address: kosai@m2.kufm.kagoshima-u.ac.jp (K. Kosai).

Abbreviations: MeCP2, methyl-CpG-binding protein 2; RTT, Rett syndrome; BDNF, brain-derived neurotrophic factor; GFAP, glial fibrillary acidic protein; ES cells, embryonic stem cells; DNs, dopaminergic neurons; TH, tyrosine hydroxylase; HPLC, high performance liquid chromatography; ACT, adenoviral conditional targeting; NSCs, neural stem cells; TTX, tetrodotoxin; TEA-Cl, tetraethylammonium-chloride; 4-AP, 4-aminopyridine; HBSS, Hanks' balanced salt solution

[1] These authors were equally contributed to this work.

0006-8993/$ – see front matter © 2010 Elsevier B.V. All rights reserved.
doi:10.1016/j.brainres.2010.08.090

1. Introduction

Rett syndrome (RTT) is a neurodevelopmental disorder that is the leading cause of mental retardation in females (Chahrour and Zoghbi, 2007). Up to 95% of classical RTT cases are caused by mutations in the methyl-CpG-binding protein 2 (MeCP2) gene, which is located at Xq28 (Amir et al., 1999). Knockout mouse models with disrupted MeCP2 function mimic many key clinical features of RTT, including normal early postnatal life followed by developmental regression resulting in motor impairment, irregular breathing and hindlimb clasping (Chen et al., 2001; Guy et al., 2001).

Although MeCP2 was previously thought to function solely as a transcriptional repressor, it was recently shown to act as both a repressor and an activator to regulate the expression of a wide range of genes (Chahrour et al., 2008). This suggests that using only genetic strategies to investigate MeCP2-related biology may be insufficient. Indeed, comparing the transcriptional profiles of whole MeCP2-deficient and wild-type mouse brains revealed subtle and non-specific transcriptional differences. In addition, although several MeCP2 target genes, including brain-derived neurotrophic factor (BDNF) and glial fibrillary acidic protein (GFAP), have been identified, the functional relevance of these genes remains largely unknown (Bienvenu and Chelly, 2006).

One of the most important but unanswered questions is the role of MeCP2 throughout various stages of neural development, particularly at early stages, including the period just prior to and at the onset of neural differentiation. However, the lack of a definitive experimental system has hampered efforts in this direction. Although anatomical studies have demonstrated that the timing of MeCP2 expression in brains is correlated with the maturation of the central nervous system, the fine spatiotemporal pattern of MeCP2 expression during early embryogenesis is largely unknown (Shahbazian et al., 2002). On the other hand, several recent studies that established and/or utilized effective cell culture systems provided valuable information on the roles of MeCP2 in the pathogenesis of RTT (Bienvenu and Chelly, 2006; Chahrour and Zoghbi, 2007). Studies on neural stem cells (NSCs) indicate that MeCP2 may play a role in neuronal maturation (Kishi and Macklis, 2004; Smrt et al., 2007). In another study, MeCP2 was shown to be involved in cell fate determination during neurogenesis (Setoguchi et al., 2006; Tsujimura et al., 2009). Moreover, two studies using an *in vitro* co-culture system have recently reported that MeCP2-deficient astroglia non-cell autonomously affected neuronal dendritic growth (Ballas et al., 2009; Maezawa et al., 2009). Whereas these studies provided important information, the role of MeCP2 throughout neural development is unknown, and in particular, the developmental abnormalities that eventually result in the onset of neurological symptoms in RTT have not yet been elucidated by conventional strategies.

RTT has been reported to be associated with abnormalities in the biogenic amine neurotransmitter/receptor systems, but these findings are controversial due to limitations of the experimental strategies used (Jellinger, 2003; Temudo et al., 2009). Some studies have demonstrated decreases in dopamine levels in the spinal fluid of human RTT patients and/or MeCP2-null animals, however, others have failed to find such changes (Ide et al., 2005; Perry et al., 1988; Samaco et al., 2009; Zoghbi et al., 1989, 1985). Pluripotent embryonic stem (ES) cells show great promise for uncovering the molecular mechanisms of development in various tissues by *in vitro* cell culture. The utility of the ES cell system for addressing a particular problem is largely determined by how efficiently the target cell type can be induced. A recent study described a co-culture system that efficiently induced mouse ES cells to differentiate into dopaminergic neurons (DNs) (Kawasaki et al., 2000). Taken together with both the present status of the controversy concerning dopaminergic abnormalities in RTT and the established experimental system that efficiently induces ES cells towards DNs, DNs may be a good candidate as a target cell type in initial studies that utilize pluripotent ES cells for analyzing functional abnormalities of MeCP2-null neurons.

Here, we develop an MeCP2-null ES cell system for analyzing developmental processes at the cellular level. We examine the role of MeCP2 in maintenance of the undifferentiated ES cell state, neuronal and glial differentiation, DN function, and neuronal maturation. We also show that MeCP2 is involved in the maturation of neurons and gliogenesis.

2. Results

2.1. *Generation of MeCP2-null ES cells by ACT*

We generated MeCP2-null and control ES cells by ACT as follows: parental ES cells (Me2loxIII16A), in which exons 3 and 4 of the Mecp2 gene on the X chromosome are flanked, were infected by Ad.Cre or control Ad.dE1.3, at a multiplicity of infection of 30 (Takahashi et al., 2006). Subsequently, the infected cells were detached and plated onto a 96-well plates at a very low concentration corresponding to less than one cell per well. Several colonies originating from isolated single cell clones were cultured and expanded in larger dishes. To generate control ES cell lines, the parental ES cells were infected with Ad.dE1.3, instead of Ad.Cre and were handled and expanded in the same way as mutant cells.

The original ES cells were derived from male E14 TG2a cell lines carrying both an X and Y chromosome (Guy et al., 2001). Genomic PCR with primer set 1 (oIMR1436 and oIMR1437) should produce a 400 bp band from hemizygous cells ($Mecp2^{-/y}$) when excision of Mecp2 exon 3 and part of exon 4 occurs, leading to the shortened and amplifiable size of this region (Fig. 1A). Non-excised DNA from parental or control ES cells is too long to be amplified by PCR using primer set 1. Primer set 2 (oIMR 1436 and oIMR 1438) can anneal and amplify only to unexcised DNA in parental or control wild-type ES cells ($Mecp2^{+/y}$) with a predicted band size of 416 bp, but cannot amplify the excised DNA due to the lack of the primer S1438 annealing site (Fig. 1A). The two selected Ad.Cre-infected clones were verified to be hemizygotes ($Mecp2^{-/y}$), in accordance with the results for Mecp2 hemizygous mice (Fig. 1B). In contrast, control ES clones infected by Ad.dE1.3 showed the wild-type band ($Mecp2^{+/y}$), in accordance with the results for wild-type mice (Fig. 1B).

We further confirmed the lack of MeCP2 mRNA expression by RT-PCR of these ES cell clones. Mecp2 has two splice isoforms, Mecp2 e1 and e2 (Kriaucionis and Bird, 2004; Mnatzakanian et al., 2004). The Ad.dE1.3-infected control ES

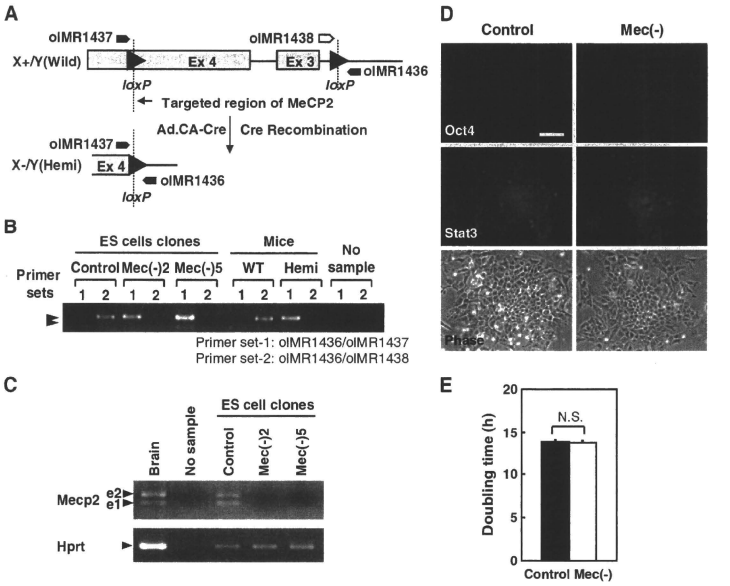

Fig. 1 – Generation and phenotypic analysis of MeCP2-null ES cells. (A) Targeted mutation of the Mecp2 locus. (B) Genotyping of control (Mecp2$^{+/Y}$) and two MeCP2-null (Mecp2$^{-/Y}$; Mec(–)) ES cell clones, and of MeCP2 wild-type and hemizygous mice was performed by PCR. Primer set 1 (oIMR 1437 and oIMR 1436) amplifies a ~400 bp mutant band, whereas primer set 2 (oIMR1438 and oIMR 1436) amplifies a 416 bp wild-type band. (C) mRNA expression of Mecp2 e1 and e2 variants in a control and two MeCP2-null ES cell clones was analyzed by RT-PCR. Wild-type mouse brain was used as a positive control. (D) The control and the MeCP2-null ES cells were stained with anti-Oct4 or anti-STAT3 antibody. Scale bar= 80 μm. (E) Doubling times of undifferentiated control and MeCP2-null ES cells are shown. N.S., no significant difference (control versus MeCP2-null ES cells, n=19 each).

cells showed expression of both Mecp2 splice variants, e1 and e2, whereas neither Mecp2 variant was detectable in both Ad. Cre-infected MeCP2-null ES cell clones (Fig. 1C). Thus, two MeCP2-null (Mecp2$^{-/Y}$) and one control (Mecp2$^{+/Y}$) ES cell clones were efficiently generated. In the following experiments, we use one of two MeCP2-null ES cell lines (clone 2) and one control ES cell line.

2.2. *Loss of MeCP2 does not appear to affect undifferentiated ES cells*

We first examined whether MeCP2 is required in undifferentiated ES cells. Prominent expression of Oct4 and Stat3, markers of the undifferentiated state, was found in the nuclei of almost all cells in both MeCP2-null and control ES cells by immunostaining (Fig. 1D). No differences in undifferentiated growth were observed between the two (Fig. 1E). Thus, MeCP2 does not appear to be critical for maintaining the undifferentiated state or for ES cell growth.

2.3. *MeCP2 is not involved in the efficiency of neural differentiation*

RT-PCR analysis showed that both Mecp2 variants, e1 and e2, were expressed in control ES cells in the undifferentiated state, as well as throughout all developmental stages (Fig. 2A).

We examined the role of MeCP2 in neuronal differentiation by comparing the phenotypes of control and MeCP2-null ES cells during differentiation. Neither the number nor the morphology of the differentiating ES colonies was significantly different between the two groups, suggesting that MeCP2 is not essential for cell growth during neural differentiation (Fig. 2B and C).

We next examined whether MeCP2 affected neuronal differentiation by immunostaining for Nestin, β-Tubulin type III (TuJ), and Tyrosine hydroxylase (TH), markers for early neuronal cells (including NSCs), differentiated neurons, and DNs, respectively (Fig. 3A–C). The percentage of Nestin-, TuJ-, and TH-positive colonies reached a maximum on day

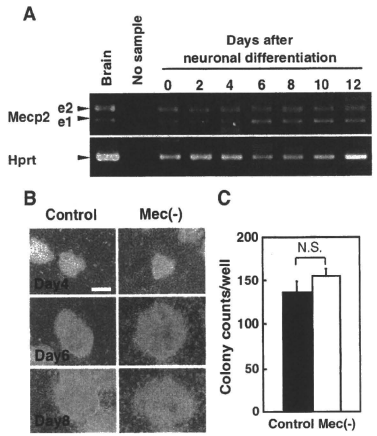

Fig. 2 – Neural differentiation of MeCP2-null ES cells. (A) mRNA expression of Mecp2 e1 and e2 variants in control ES cells on the indicated days after the start of co-culture on PA6 cells was analyzed by semi-quantitative RT-PCR. Wild-type mouse brain was used as a positive control. (B) Representative images of control and MeCP2-null ES cell colonies on the indicated days after co-culture on PA6 cells. Scale bar=200 μm. (C) The number of colonies per well was counted on day 10.

8 and did not differ between the two groups. Thus, loss of MeCP2 does not affect the efficiency of neuronal differentiation. The percentage of Nestin-, TuJ-, and TH-positive MeCP2-null colonies was higher than that of control colonies on day 4, and the percentage of Nestin-positive MeCP2-null colonies on day 12 was lower than that of the controls, although the slightly precocious differentiation was not significant. The results suggest that MeCP2 is not essential for induction of neuronal differentiation, at least induction toward DNs.

2.4. *Loss of MeCP2 causes immature resting and active membrane properties in ES cell-derived neurons*

To analyze neuronal maturity, the membrane properties of control and MeCP2-null ES cell-derived neurons were examined by electrophysiology on days 10–12 (Table 1). The peak current densities of the voltage-dependent Na^+ currents (I_{Na}s) underlying the rising phase of the action potential and the A-type K^+ currents (I_As) were significantly smaller in the MeCP2-null ES cell-derived neurons than in the controls (Fig. 4A and B). In contrast, the peak currents of the delayed rectifier K^+ currents (I_{DR}s) did not significantly differ between the control and MeCP2-null ES cell-derived neurons (Fig. 4C). In addition, the repetitive spikes showed a relatively high firing frequency and rundown in amplitude in the MeCP2-null ES cell-derived neurons (Fig. 4D). The rundown may be due to a decrease in expression of I_{Na}s and the I_As. These results suggest that MeCP2 contributes to the development of resting and active membrane properties, and that MeCP2-null ES cell-derived neurons do not reach maturity.

2.5. *MeCP2 does not appear to affect dopaminergic function*

To examine the involvement of MeCP2 in DN function, dopamine production and release were investigated by reverse phase HPLC in MeCP2-null and control ES cell-derived neurons on day 10 of culture. In response to a depolarizing stimulus, DNs derived from MeCP2-null ES cells released as much dopamine into the medium as did control cells (Fig. 5). Thus, MeCP2 is not critical for the dopaminergic function of DNs, at least in this experimental system.

2.6. *MeCP2 deficiency accelerates glial differentiation*

Because interactions between neurons and glia are essential for the development and function of neurons (Corbin et al., 2008; Stevens, 2008), we examined changes in expression of the glial marker GFAP in ES colonies during neural differentiation. GFAP-positive colonies emerged earlier and were present at a higher percentage on days 8 and 12 in MeCP2-null ES cells compared to controls (Fig. 6A and B), consistent with the GFAP expression observed in colonies (Fig. 6C). The significantly accelerated glial differentiation in MeCP2-deficient cells suggests that MeCP2 negatively regulates glial differentiation. In addition, the timing of differentiation, with the start of neuronal differentiation preceding the start of glial differentiation, as well as the presence of both neurons and glia in differentiated ES colonies mirror normal neural development (Qian et al., 2000; Stevens, 2008), underscore the usefulness of this experimental system.

3. Discussion

The overall role of MeCP2 throughout neural development, particularly at early stages before the onset of neural differentiation, has not been investigated due to the lack of a definitive experimental system or materials. In this study, we first demonstrated that MeCP2-null ES cell could be feasibly generated by applying the *in vitro* ACT method to loxP-floxed ES cells that were originally engineered for a generation of conditional knockout mouse (Takahashi et al., 2006). Just as there were no significant adverse effects from ACT on cell cycle regulation, cell viability, or the efficiency of differentiation in ES cells, the MeCP2-null and the control ES cells generated by ACT worked with no problems in several types of experiments in the previous and the present study (Takahashi et al., 2006). In addition, the co-culture method that was used in the present study has the advantages of both technical feasibility and high efficiency of dopaminergic differentiation (Kawasaki et al., 2000). Our experimental system of comparing MeCP2-null and control ES cells throughout their developmental stages, including in the undifferentiated state and at the early stage of neural development, provided important information about the role of MeCP2 in neural development.

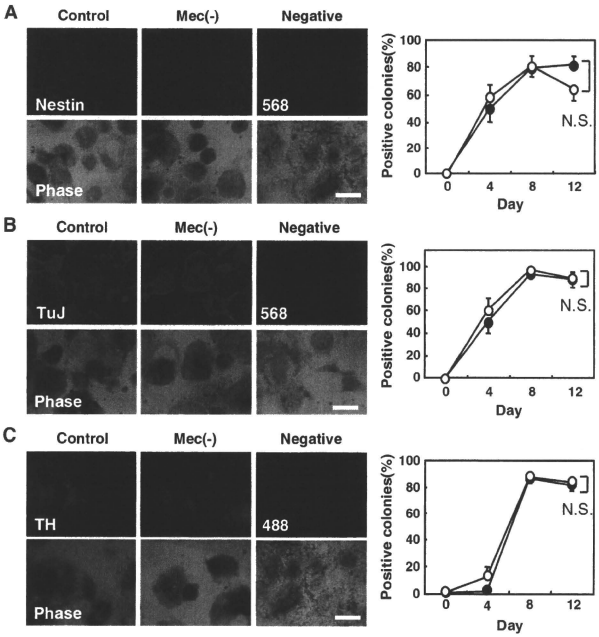

Fig. 3 – Neuronal differentiation of MeCP2-null ES cells. (A–C) Control (closed circle) and MeCP2-null (open circle) ES cells on days 4, 8, and 12 were stained with antibody against Nestin (A), TuJ (B), or TH (C). Negative control indicates colonies on day 12 that were stained with only the secondary Alexa Fluor 488 or 568 antibodies without primary antibodies. N.S., no significant difference (control versus MeCP2-null ES cells at each time point). Between 50 and 200 colonies per well were counted to calculate the mean ± SD (Nestin; $n = 5$, TuJ; $n = 5$, and TH; $n = 3$) and the results were verified in three different experiments. Representative images from day 12 are shown on the left. Scale bar = 0.5 mm.

Using this system, we have clarified several important issues, some of which are consistent with previous findings. First, we demonstrated that MeCP2 is not essential for the maintenance or growth of undifferentiated ES cells, supporting the previous finding that absence of MeCP2 did not cause embryonic lethality in mice (Guy et al., 2001). Second, MeCP2 deficiency has a minimal effect on neurogenesis, consistent with the fact that the brains of RTT patients and MeCP2-null mice are morphologically and phenotypically normal at birth (Armstrong, 2002; Chahrour and Zoghbi, 2007). Thus, MeCP2 is likely not an essential part of the machinery that advances neurogenesis. On the other hand, while it has been reported that MeCP2 was involved in neuronal maturation rather than cell fate decisions (Kishi and Macklis, 2004; Smrt et al., 2007), the present results suggested that MeCP2 was remarkably somewhat involved in negative regulation of glial differentiation and neuronal maturation. Apparently inconsistent results between the previous and present studies may be due to the difference in experimental systems. For instance, MeCP2 was expressed in neurons and undifferentiated neuroepithelial cells at high and almost undetectable levels, respectively, in the experimental system of the previous study (Kishi and Macklis, 2004), whereas in the present system MeCP2 expressions were clearly detected in not only ES cell-derived differentiated neurons but also in undifferentiated ES cells. This aspect of the present experimental system may have the advantage of being able to sensitively and carefully detect any possible phenotypes in order to determine whether MeCP2 affects neural development, including gliogenesis, during any stage, including early stages before the onset of neural differentiation.

In contrast, MeCP2-null ES-derived neurons are electrophysiologically immature, suggesting that MeCP2 contributes to the development of the active membrane properties. Biella et al. have reported that voltage-gated Na^+ currents gradually increase during neuronal maturation, but that I_{DR}s is already

Table 1 – Differences in electrophysiological parameters between control and MeCP2-null ES-derived cells.

	Parameters	Control	Mec(–)
I_{Na}	Peak amplitude, pA	−1060±140(4)	−701.8±184.9(5)*
	Current density, pA/pF	−96.4±6.5(4)	−64.2±8.7(5)*
I_A	Peak amplitude, pA	89.0±32.2(4)	30.1±8.4(4)*
	Current density, pA/pF	8.3±1.7(4)	3.0±0.7(4)*
I_{DR}	Peak amplitude, pA	169.2±87.1(3)	105.7±53.4(4)
	Current density, pA/pF	15.8±7.2(3)	11.0±7.2(4)
	Membrane capacitance, pF	10.7±1.6(11)	10.3±1.8(13)
	V_{Rm}, mV	−52.8±11.4(6)	−52.1±10.7(7)
	Threshold, mV	−44.4±4.9(6)	−37.6±1.0(6)*
	Firing frequency, Hz	5.8±1.0(6)	9.3±0.8(6)*

I_{Na}; voltage-dependent Na^+ current, I_A; A-type K^+ current, I_{DR}; delayed rectifier K^+ current, V_{Rm}; resting membrane potential
Numbers in parentheses indicate the recording cell number.
Firing frequency is derived from mean firing rate during the injection of depolarizing current of which amplitude is two times of the threshold.
* Indicates statistical significance between the control and the MeCP2-null ES-derived neurons by Student's test with $p<0.05$.

at a mature state at early stages of neural development in ES-derived NSCs (Biella et al., 2007). The amplitude of I_As also increases during the late embryonic-early postnatal developmental period in hippocampal neurons (Ficker and Heinemann, 1992). Thus, MeCP2 may be required for neuronal maturation (development of voltage-gated Na^+ currents and I_As), suggesting that some neuronal symptoms in RTT may be caused by immature neuronal membrane properties.

In terms of the neural immaturity in MeCP2-deficient cultures, it should be noted that loss of MeCP2 led to drastically increased gliogenesis. The involvement of MeCP2 in gliogenesis may be supported by previous studies, although their data were indirect and limited to middle and late phases of neural development (Deguchi et al., 2000; Nagai et al., 2005; Setoguchi et al., 2006). For instance, inhibition of MeCP2 in E18 non-neuronal mouse cells inhibited cell growth (Nagai et al., 2005), and ectopic overexpression of MeCP2 inhibited E14.5 neuroepithelial cells from differentiating into GFAP-positive cells (Setoguchi et al., 2006). Moreover, MeCP2 binds to a highly methylated region in the GFAP promoter. Thus, the authors suggested that MeCP2 is involved in restricting differentiation

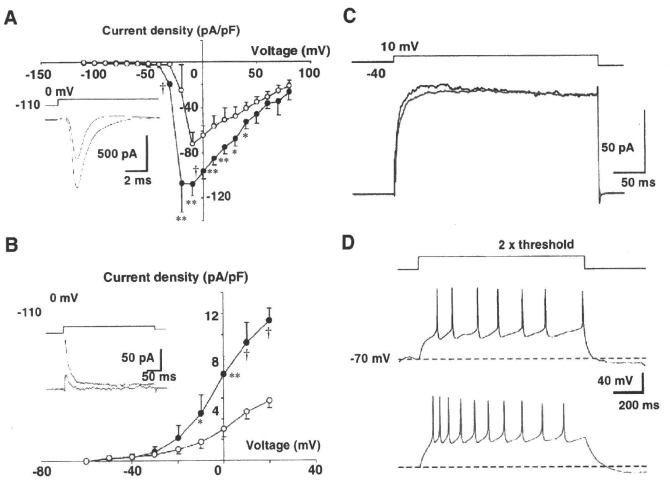

Fig. 4 – Electrophysiological analysis of control and MeCP2-null ES cell-derived neurons. (A) Voltage-dependent Na^+ currents (I_{Na}s) were recorded from control and MeCP2-null ES cell-derived neurons on days 10–12. Current density–voltage (I–V) relationships were obtained from control ($n=4$, closed circles) and MeCP2-null neurons ($n=5$, open circles). Inset traces show the mean I_{Na}s elicited by the voltage step pulse from −110 to 0 mV in control (black, $n=4$) and MeCP2-null neurons (red, $n=5$). Symbols for statistical significance: *$P<0.05$; **, $P<0.01$; and †$P<0.001$ (control versus MeCP2-null neurons). (B) Fast inactivating K^+ currents (I_As) were recorded from control and MeCP2-null neurons. I–V relationships were obtained from control ($n=4$, closed circles) and MeCP2-null neurons ($n=4$, open circles). Inset traces show the mean I_As elicited by the voltage step pulse from −110 to 0 mV. (C) Sustained K^+ currents (I_{DR}s) were recorded from control (black, $n=3$) and MeCP2-null neurons (red, $n=4$). Each trace shows the mean I_{DR}s elicited by the voltage step pulse from −40 to +10 mV. (D) Response to the depolarizing current pulse injection of membrane was recorded from control (black, $n=6$) and MeCP2-null neurons (red, $n=6$). In each trace, the dashed line indicates the holding membrane potential (−70 mV), and upward deflections during the current pulse injection indicate Na^+ spikes.

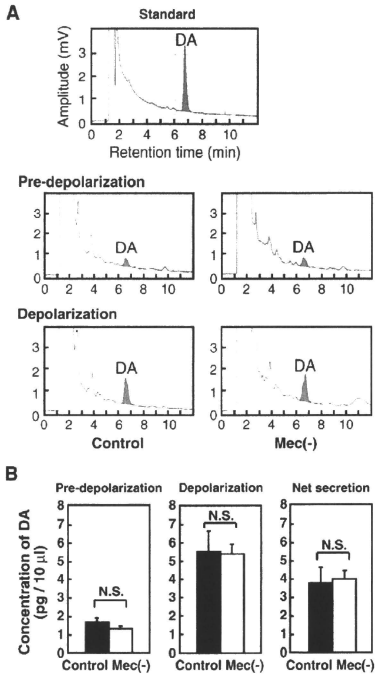

Fig. 5 – Dopamine production and release in MeCP2-null ES cell-derived DNs. (A) Dopamine releases in the media of control and MeCP2-null ES cells on day 10 were analyzed by reverse phase HPLC. The standard panel shows chromatography of a standard solution. DA indicates peaks of dopamine. The retention time for dopamine was 6.5 min in each case. (B) The graphs represent the quantitative HPLC data for dopamine secretion. Dopamine secretion was measured in samples incubated for 15 min with HBSS (pre-depolarization) or high K^+ HBSS (depolarization). Pre-depolarization indicates the spontaneous secretion of dopamine. Net secretion is the depolarized peak release minus the spontaneous dopamine release and shows the response in the presence of potassium. N.S., no significant difference (control versus MeCP2-null ES cells, $n=8$ each).

plasticity in neurons, possibly by stage-specific and neuron-specific methylation of glial genes (Setoguchi et al., 2006).

Interestingly, brain magnetic resonance in MeCP2-null mice demonstrated that metabolism in both neurons and glia was affected (Saywell et al., 2006). In addition, a study using *in vitro* co-culture system has recently demonstrated that MeCP2 mutant astrocytes and their conditioned medium failed to support normal dendritic morphology of hippocampal neurons, suggesting that MeCP2-deficient astrocytes have a non-cell autonomous effect on neuronal properties (Ballas et al., 2009; Maezawa et al., 2009). In general, the coordinated interactions between glia and neurons are crucial for normal neuronal development and function (Allen and Barres, 2009; Corbin et al., 2008; Stevens, 2008). Together with previous data, our results suggest that the main physiological role of MeCP2 in neural development is the inhibition of gliogenesis, and that distorted interactions with abnormally developed glia result in electrophysiologically immature neurons.

Finally, this study may at least in part resolve some of the controversy over whether or not abnormalities in biogenic amine neurotransmitter/receptor systems are associated with RTT (Matsuishi et al., 2001; Temudo et al., 2009; Wenk, 1995). Discrepancies between different studies may be due to the limitations of the experimental strategies, which involved clinical examination of dopamine levels in central spinal fluid, dopamine D2 receptors, or pathological alterations in symptomatic RTT patients (Chiron et al., 1993; Lekman et al., 1990; Perry et al., 1988; Zoghbi et al., 1989, 1985). Here, we demonstrate that MeCP2 is involved in neither the differentiation nor the dopamine production and release of DNs. This has important clinical implications, since whatever abnormalities might exist in the dopaminergic system in RTT patients, they are not directly related to defects in the DNs themselves. However, a potential limitation of the present study is that the ES cell-derived DNs might not be entirely equivalent to DNs in adolescent RTT patients, even though almost all the ES cell colonies were TH-positive. Using this experimental system to uncover the cellular and molecular characteristics of MeCP2-null DNs, in conjunction with studies of MeCP2-null mice and clinical examination of RTT patients, will answer this question definitively in the future.

In conclusion, we have developed an *in vitro* system for analyzing neuronal development and the function of MeCP2. We found that MeCP2 is not essential for maintaining the undifferentiated ES cell state, for neurogenesis, or for DN function; rather, it is mainly involved in inhibiting gliogenesis. Imperfect neuronal maturity, probably resulting from abnormal gliogenesis, may be involved in the pathogenesis of RTT. All the information is useful not only for understanding the developmental roles of MeCP2 and the pathogenesis of RTT, but also for developing therapeutic strategies for RTT in the future.

4. Experimental procedures

4.1. *Recombinant adenoviral vectors*

E1-deleted, replication-deficient adenoviral vector expressing Cre under the transcriptional control of the cytomegalovirus early enhancer and chicken beta-actin promoter (Ad.Cre) or no gene (Ad.dE1.3) was prepared as described previously (Chen et al., 1995; Takahashi et al., 2006).

4.2. *ES cell culture and ACT*

Mouse ES cells in which exons 3 and 4 of Mecp2 were flanked by loxP sites, and which were previously used to generate

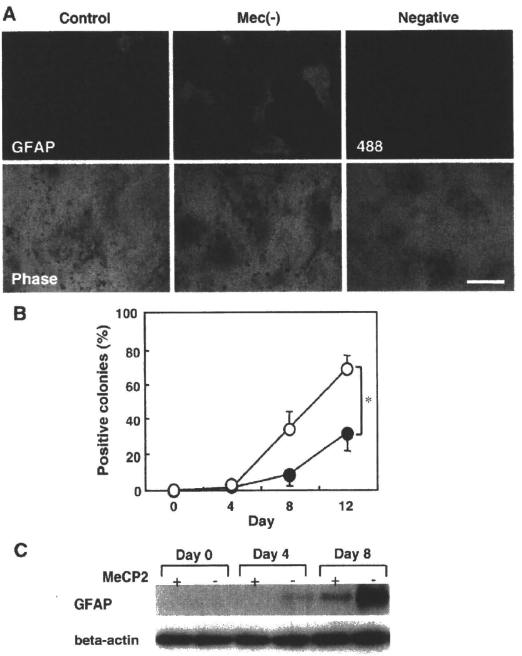

Fig. 6 – Glial differentiation of MeCP2-null ES cells. Control or MeCP2-null ES cell colonies 4, 8, and 12 days after co-culture on PA6 cells were immunostained for GFAP. (A) The top and bottom pictures show immunofluorescent microscopic and phase-contrast observations of ES colonies, respectively, which were stained with an anti-GFAP (green) antibody on day 12. Negative control images show colonies stained with the secondary Alexa Fluor 488 antibody on day 12. Scale bar = 0.5 mm. (B) The graph shows the percentage of control (closed circle) and MeCP2-null (open circle) GFAP-positive ES cell colonies on the indicated days. *$P<0.05$ (control versus MeCP2-null ES cells, $n=5$ each, 50–200 colonies per well). Data are means ± SD for three separate measurements from different experiments. (C) Expressions of GFAP protein in control and MeCP2-null ES cells on the indicated days were analyzed by Western blot. Beta-actin protein levels were analyzed in the same way as an internal control.

MeCP2-null mice, were provided by Dr. A. Bird (Guy et al., 2001). ES cells were maintained in the undifferentiated state without feeder cells on gelatin-coated dishes in Glasgow Minimum Essential Medium (G-MEM, GIBCO/BRL, Grand Island, NY, USA) supplemented with 10% fetal bovine serum (FBS), 2 mM L-glutamine (GIBCO/BRL), 1 mM pyruvate (GIBCO/BRL), 0.05 mM 2-mercaptoethanol (2-ME, Nacalai Tesque, Inc., Kyoto, Japan), 0.1 mM nonessential amino acids (GIBCO/BRL), and 2000 U/ml leukemia inhibitory factor (ESGRO, Chemicon International, Temecula, CA) as previously described (Guy et al., 2001; Kawai et al., 2004; Takahashi et al., 2006). MeCP2-null and control ES cells were generated by the ACT method using Ad.Cre and Ad.dE1.3, respectively (Chen et al., 1995; Takahashi et al., 2006). Details are described in the Results section.

Doperminergic neurons were induced essentially as previously described, with some modifications (Kawasaki et al., 2000; Takahashi et al., 2006). Briefly, 1000 MeCP2-null or control ES cells were placed on feeder PA6 cells that had been seeded on collagen-coated eight-well glass plates. Subsequently, these ES cells were co-cultured with PA6 cells in differentiation medium, which consists of G-MEM supplemented 10% knockout serum replacement (KSR, GIBCO/BRL), 2 mM L-glutamine, 1 mM pyruvate, 0.1 mM nonessential amino acids, and 0.1 mM 2-mercaptoethanol as described previously (Kawasaki et al., 2000). The differentiation medium was changed on day 4 and every other day thereafter. After 8 days in differentiation medium, cells were cultured in G-MEM supplemented with N2 (GIBCO/BRL), 100 mM

tetrahydrobiopterin, 200 mM ascorbate, 1 mM pyruvate, 0.1 mM nonessential amino acids, and 0.1 mM 2-mercaptoethanol.

4.3. *Animals*

The tails of MeCP2-null mice were used as positive controls for genomic PCR (Fig. 1B) in accordance with a protocol approved by the Animal Research Committee of Kurume University and the National Institutes of Health Guidelines for the Care and Use of Laboratory Animals.

4.4. *PCR analysis*

Genomic DNA was extracted from ES cells and PCR genotyping was performed on genomic DNA using oIMR1436, oIMR1437, and oIMR1438 primers and the protocol provided by the manufacturer (http://jaxmice.jax.org/pub-cgi/protocols/protocols.sh?objtype=protocol&protocol_id=598) (Fig. 1A) (Guy et al., 2001).

Extraction of total RNA, RT-PCR analysis, and electrophoresis were carried out as described previously (Kawai et al., 2004; Takahashi et al., 2006). PCR conditions were as follows: 40 cycles of 94 °C for 30 s, 61 °C for 60 s, and 74 °C for 60 s, using the mouse Mecp2 exon-specific primers 5′-GGTAAAACCCGTCCG GAAAATG-3′ (sense) and 5′-TTCAGTGGCTTGTCTCTGAG-3′ (antisense) (Kriaucionis and Bird, 2004).

4.5. *Immunocytochemistry*

Cells were stained using antibodies against Nestin (dilution 1:100, clone 25, BD Biosciences Pharmingen, San Diego, CA), Tyrosine hydroxylase (TH) (dilution 1:100, clone AB152, Chemicon International), β-Tubulin type III (dilution 1:500, TuJ, Sigma-Aldrich, Inc., St. Louis, MO), GFAP (dilution 1:500, clone G-A-5, Sigma-Aldrich, Inc.), Oct-4 (dilution 1:500, clone C-10, Santa Cruz Biotechnology, Inc., Santa Cruz, CA), or Stat-3 (dilution 1:500, C-20, Santa Cruz Biotechnology, Inc.), together with secondary fluorescent antibodies (dilution 1:500) as described previously (Kawai et al., 2004; Takahashi et al., 2006). As a negative control, cells were stained with only secondary fluorescent antibodies without primary antibodies (Figs. 3, 6A, and Suppl. Fig. 1).

4.6. *Immunoblotting*

Protein was extracted from ES cells and Western blot analysis was performed using anti-GFAP (clone G-A-5) and anti-Actin (clone AC-40, Sigma-Aldrich, Inc.) monoclonal antibodies, and detected with horseradish peroxidase-conjugated anti-mouse IgG (DakoCytomation, Glostrup, Denmark) and chemiluminescent substrate (Chemi-Lumi One, Nacalai Tesque, Inc.), as described previously (Takahashi et al., 2006).

4.7. *Electrophysiological analysis*

Electrophysiological measurements were performed as described previously (Murai and Akaike, 2005). Briefly, whole cell patch-clamp recordings were made from 29 ES cell-derived neurons with glass patch-pipettes. The resistance of patch electrodes was 4–8 MΩ. Cells were voltage or current clamped. The membrane currents or potentials were measured with a patch-clamp amplifier (Axopatch 200A, Axon Instruments Inc., Union City, CA, USA). Whole cell currents or membrane potentials were low-pass filtered at 1–2 kHz, digitized at a sampling rate of 20 kHz, and stored on a computer hard disc (pCLAMP 8, Axon Instruments Inc.). Series resistance was compensated by 50–70%. All experiments were performed at room temperature (21–24 °C).

The membrane was first held at −110 mV and then depolarized by voltage step pulses (300 ms duration) from −110 to +80 mV with 10 mV steps to elicit the membrane currents. In the absence and presence of voltage-dependent Na^+ channel blocker, tetrodotoxin (TTX, 300 nM), the total membrane currents and TTX resistant (TTX-R) currents were obtained, respectively. The voltage-dependent sodium (Na^+) current, which is TTX sensitive (TTX-S), was obtained by subtracting the TTX-R currents from the total membrane currents in both the control and MeCP2-null ES cell-derived neurons.

Two types of voltage-dependent potassium (K^+) currents were also recorded in both the control and the MeCP2-null ES cell-derived neurons: fast inactivating K^+ current (A-type K^+ current, I_A) and sustained K^+ current (delayed rectifier K^+ current, I_{DR}), sensitive to 4-aminopyridine (4-AP, 1 mM) and tetraethylammonium-chloride (TEA-Cl, 20 mM), respectively. The voltage step pulse from −110 to +20 mV with 10 mV step (300 ms duration) in the presence of TTX (300 nM) elicited the combined membrane K^+ currents. To obtain I_{DR}, the membrane was first held at −40 mV and then depolarized from −40 to +20 mV with 10 mV steps (300 ms duration), because I_A inactivated at −40 mV and I_{DR} was activated from −40 mV. Subtraction of I_{DR} from the combined membrane K^+ currents yielded I_A.

In current-clamp recording, injection of the depolarizing current pulse (2 ms, 0.15–0.20 nA) elicited an action potential just after the end of the current injection. In both control and MeCP2-null ES cell-derived neurons, injection of a prolonged depolarizing current pulse (1 s duration and two times the intensity for the threshold) elicited repetitive firings during membrane depolarization.

4.8. *High performance liquid chromatography (HPLC)*

To measure dopamine content and secretion in MeCP2-null and control ES cells that were differentiated into DNs on PA6 cells for 10 days, an HPLC electrochemical detector (ECD) system (HTEC-500, Eicom Corp., Kyoto, Japan) was used in accordance with the manufacturer's protocol, with some modifications (Kawasaki et al., 2000). Briefly, ES cells cultured in six-well plates were washed twice with Hanks' balanced salt solution (HBSS), then incubated for 15 min in high K^+ (56 mM) HBSS to evoke membrane depolarization. The incubation buffer (a 500 ml aliquot) was collected and centrifuged at 800×*g* for 10 min to remove detached cells, and the 400 ml supernatant was mixed with 400 ml of 20 mM hydrochloric acid and 100 mM EDTA. Ten microliters of each sample was injected into the HPLC-ECD system and separated with a reverse phase column (Eicompak CA-50DS, Eicom) using 0.1 M phosphate buffer (pH 6.0) containing 2.3 mM 1-octanesulfonic acid, 0.13 mM EDTA, and 20% methanol as a

mobile phase at a flow rate of 0.23 ml/min. The retention time for dopamine was 6–8 min. The amount of dopamine in each sample was calculated by using the peak height ratio relative to the standard dopamine hydrochloride (H8502, Sigma-Aldrich, Inc.) solution.

4.9. *Statistical analysis*

Quantitative results are expressed as means±SD. The Student's *t*-test was used to compare data, with $p<0.05$ considered significant.

Supplementary materials related to this article can be found online at doi:10.1016/j.brainres.2010.08.090.

Competing interests statement

The authors declare that they have no competing financial interests.

Acknowledgments

This work was supported in part by a project for establishing open research centers in private universities, a Grant-in-Aid for Scientific Research (B) and a Grant-in-Aid for Young Scientists (B) from the Japan Society for the Promotion of Science, and by a Grant from Terumo Life Science Foundation. We would like to thank Adrian Bird for providing the MeCP2 targeted ES cells; and Kaori Noguchi, Chikako Goto, and Aya Niihara for technical assistance.

REFERENCES

Allen, N.J., Barres, B.A., 2009. Neuroscience: Glia—more than just brain glue. Nature 457, 675–677.

Amir, R.E., Van den Veyver, I.B., Wan, M., Tran, C.Q., Francke, U., Zoghbi, H.Y., 1999. Rett syndrome is caused by mutations in X-linked MECP2, encoding methyl-CpG-binding protein 2. Nat. Genet. 23, 185–188.

Armstrong, D.D., 2002. Neuropathology of Rett syndrome. Ment. Retard. Dev. Disabil. Res. Rev. 8, 72–76.

Ballas, N., Lioy, D.T., Grunseich, C., Mandel, G., 2009. Non-cell autonomous influence of MeCP2-deficient glia on neuronal dendritic morphology. Nat. Neurosci. 12, 311–317.

Biella, G., Di Febo, F., Goffredo, D., Moiana, A., Taglietti, V., Conti, L., Cattaneo, E., Toselli, M., 2007. Differentiating embryonic stem-derived neural stem cells show a maturation-dependent pattern of voltage-gated sodium current expression and graded action potentials. Neuroscience 149, 38–52.

Bienvenu, T., Chelly, J., 2006. Molecular genetics of Rett syndrome: when DNA methylation goes unrecognized. Nat. Rev. Genet. 7, 415–426.

Chahrour, M., Zoghbi, H.Y., 2007. The story of Rett syndrome: from clinic to neurobiology. Neuron 56, 422–437.

Chahrour, M., Jung, S.Y., Shaw, C., Zhou, X., Wong, S.T., Qin, J., Zoghbi, H.Y., 2008. MeCP2, a key contributor to neurological disease, activates and represses transcription. Science 320, 1224–1229.

Chen, R.Z., Akbarian, S., Tudor, M., Jaenisch, R., 2001. Deficiency of methyl-CpG binding protein-2 in CNS neurons results in a Rett-like phenotype in mice. Nat. Genet. 27, 327–331.

Chen, S.H., Chen, X.H., Wang, Y., Kosai, K., Finegold, M.J., Rich, S.S., Woo, S.L., 1995. Combination gene therapy for liver metastasis of colon carcinoma in vivo. Proc. Natl. Acad. Sci. U. S. A. 92, 2577–2581.

Chiron, C., Bulteau, C., Loc'h, C., Raynaud, C., Garreau, B., Syrota, A., Maziere, B., 1993. Dopaminergic D2 receptor SPECT imaging in Rett syndrome: increase of specific binding in striatum. J. Nucl. Med. 34, 1717–1721.

Corbin, J.G., Gaiano, N., Juliano, S.L., Poluch, S., Stancik, E., Haydar, T.F., 2008. Regulation of neural progenitor cell development in the nervous system. J. Neurochem. 106, 2272–2287.

Deguchi, K., Antalffy, B.A., Twohill, L.J., Chakraborty, S., Glaze, D.G., Armstrong, D.D., 2000. Substance P immunoreactivity in Rett syndrome. Pediatr. Neurol. 22, 259–266.

Ficker, E., Heinemann, U., 1992. Slow and fast transient potassium currents in cultured rat hippocampal cells. J. Physiol. 445, 431–455.

Guy, J., Hendrich, B., Holmes, M., Martin, J.E., Bird, A., 2001. A mouse Mecp2-null mutation causes neurological symptoms that mimic Rett syndrome. Nat. Genet. 27, 322–326.

Ide, S., Itoh, M., Goto, Y., 2005. Defect in normal developmental increase of the brain biogenic amine concentrations in the mecp2-null mouse. Neurosci. Lett. 386, 14–17.

Jellinger, K.A., 2003. Rett syndrome—an update. J. Neural Transm. 110, 681–701.

Kawai, T., Takahashi, T., Esaki, M., Ushikoshi, H., Nagano, S., Fujiwara, H., Kosai, K., 2004. Efficient cardiomyogenic differentiation of embryonic stem cell by fibroblast growth factor 2 and bone morphogenetic protein 2. Circ. J. 68, 691–702.

Kawasaki, H., Mizuseki, K., Nishikawa, S., Kaneko, S., Kuwana, Y., Nakanishi, S., Nishikawa, S.I., Sasai, Y., 2000. Induction of midbrain dopaminergic neurons from ES cells by stromal cell-derived inducing activity. Neuron 28, 31–40.

Kishi, N., Macklis, J.D., 2004. MECP2 is progressively expressed in post-migratory neurons and is involved in neuronal maturation rather than cell fate decisions. Mol. Cell. Neurosci. 27, 306–321.

Kriaucionis, S., Bird, A., 2004. The major form of MeCP2 has a novel N-terminus generated by alternative splicing. Nucleic Acids Res. 32, 1818–1823.

Lekman, A., Witt-Engerstrom, I., Holmberg, B., Percy, A., Svennerholm, L., Hagberg, B., 1990. CSF and urine biogenic amine metabolites in Rett syndrome. Clin. Genet. 37, 173–178.

Maezawa, I., Swanberg, S., Harvey, D., LaSalle, J.M., Jin, L.W., 2009. Rett syndrome astrocytes are abnormal and spread MeCP2 deficiency through gap junctions. J. Neurosci. 29, 5051–5061.

Matsuishi, T., Yamashita, Y., Kusaga, A., 2001. Neurobiology and neurochemistry of Rett syndrome. Brain Dev. 23 (Suppl 1), S58–S61.

Mnatzakanian, G.N., Lohi, H., Munteanu, I., Alfred, S.E., Yamada, T., MacLeod, P.J., Jones, J.R., Scherer, S.W., Schanen, N.C., Friez, M.J., Vincent, J.B., Minassian, B.A., 2004. A previously unidentified MECP2 open reading frame defines a new protein isoform relevant to Rett syndrome. Nat. Genet. 36, 339–341.

Murai, Y., Akaike, T., 2005. Orexins cause depolarization via nonselective cationic and K+ channels in isolated locus coeruleus neurons. Neurosci. Res. 51, 55–65.

Nagai, K., Miyake, K., Kubota, T., 2005. A transcriptional repressor MeCP2 causing Rett syndrome is expressed in embryonic non-neuronal cells and controls their growth. Brain Res. Dev. Brain Res. 157, 103–106.

Perry, T.L., Dunn, H.G., Ho, H.H., Crichton, J.U., 1988. Cerebrospinal fluid values for monoamine metabolites, gamma-aminobutyric acid, and other amino compounds in Rett syndrome. J. Pediatr. 112, 234–238.

Qian, X., Shen, Q., Goderie, S.K., He, W., Capela, A., Davis, A.A., Temple, S., 2000. Timing of CNS cell generation: a programmed sequence of neuron and glial cell production from isolated murine cortical stem cells. Neuron 28, 69–80.